Measurements of the Diffusion and Reflection Coefficients of Cd($^1S_0$) in Noble Gases

P. Rudecki and J. Domysławska

Institute of Physics, Nicolaus Copernicus University
Grudziądzka 5, 87-100 Toruń, Poland

(Received June 2, 2003; revised version September 17, 2003)

A new method of simultaneous determining of the diffusion coefficient and the reflection coefficient of atoms from the reservoir walls is presented. The diffusion coefficient of cadmium atoms in the ground state in buffer noble gas atoms such as Ne, Ar, Kr, and Xe and reflection coefficient of Cd atoms from the quartz cell wall in the temperature range 350–550 K were determined. Experimental values of diffusion coefficient are compared with theoretical ones calculated from available potentials.

PACS numbers: 82.56.Lz, 34.50.Dy, 34.90.+q

1. Introduction

The knowledge of the diffusion coefficient of metal atoms in gases is of importance in various plasma devices and metal vapour lasers especially hardly melting metal lasers [1–4]. Diffusion of metal atoms in gases plays also an important role in studies of light-induced drift of atoms in a gas as well as the influence of velocity changing collisions on the shapes of pressure-broadened spectral lines. Determination of the diffusion coefficient of metal atoms in gases is still connected with severe experimental difficulties and this explains the fact that only a limited number of experimental data is available in the literature. Most measurements have been done using optical methods in which the gradient of densities is produced in a pulsed hollow cathode discharge [1, 3–5]. In a method given by Cornelissen [6] a pulsed glow discharge is used to create the gradient in a cell.

This paper deals with the diffusion of cadmium atoms in noble gases and was stimulated by recent experiment study on the role of Dicke narrowing in the formation of collisionally-perturbed shape of the Cd 326.1 nm intercombination line [7]. We have used the Cornelissen method and modified it in such a way that the gradient of cadmium densities in a cylindrical cell was produced due to electrodeless high frequency discharge. After termination of the high-frequency field the absorption of the Cd resonance line ($^1S_0$–$^3P_1$) was registered. The absorption signal was then fitted by a few diffusion modes of the solution of the diffusion equation. This method was recently applied [8] to determine the diffusion coefficient of cesium atom in helium and argon.

2. Theoretical foundations

We assume the cylindrical symmetry of the discharge region as presented in Fig. 1. Using the cylindrical coordinates r, z, φ the density $n = n(r, z, t)$ of the cadmium atoms is determined by the diffusion equation

$$\frac{\partial n}{\partial t} = D\left[\frac{\partial^2 n}{\partial r^2} + \frac{1}{r}\frac{\partial n}{\partial r} + \frac{\partial^2 n}{\partial z^2}\right], \tag{1}$$

where r is the radial distance from the axis, and D is the diffusion constant.

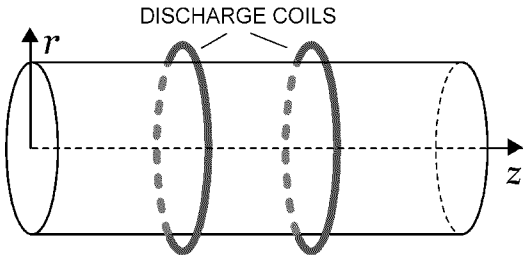

Fig. 1. Geometry of the discharge coils and the cell.

Equation (1) should be solved with the third kind boundary conditions commonly used in the kinetic theory of stochastic processes in gaseous systems and their interaction with surfaces [5, 9–11] which are given by

$$\frac{\partial n(r, z, t)}{\partial z}|_{z=0} = \alpha_1 n(r, z, t)|_{z=0}, \tag{2}$$

$$\frac{\partial n(r, z, t)}{\partial z}|_{z=l_0} = -\alpha_2 n(r, z, t)|_{z=l_0}, \tag{3}$$

$$\frac{\partial n(r, z, t)}{\partial r}|_{r=r_0} = -\alpha_3 n(r, z, t)|_{r=r_0}, \tag{4}$$

where l_0 is the length of cylindrical cell and r_0 is the radius of the cell. The magnitudes α_1, α_2, and α_3 fulfill the following condition [12]:

$$\alpha_1 = \alpha_2 = \alpha_3 \equiv \alpha = \frac{1-R}{1+R}\,\frac{1}{\lambda\cos\vartheta}, \tag{5}$$

where R is the reflection coefficient of the Cd atom from the surface, λ is the mean free path and $\cos\vartheta$ expresses the mean projection of the flux of particles on the direction perpendicular to the surface of the reservoir. In the kinetic theory it is usually assumed that $\cos\vartheta = 2/3$. Masnou-Seeuws and Bouchiat [10] and Chantry [11] have shown that for $\cos\vartheta = 2/3$ the boundary conditions (2–4) lead to asymptotically correct solution of the diffusion equation, i.e. in the case when the mean free path becomes of the order of the reservoir dimension.

In the case of axial symmetry the solution $n = n(r,z,t)$ of the diffusion equation (1) fulfilling the boundary conditions (2–5) can be written in the form

$$n(r,z,t) = n_0 + \sum_{m,j} A_{mj} J_0\left(\frac{\mu_j}{r_0} r\right) \sin\left(\frac{\nu_m}{l_0} z + \eta_m\right) \exp\left(-D\beta_{mj} t\right), \tag{6}$$

where n_0 is the density of cadmium atoms at equilibrium and

$$\beta_{mj} = \left(\frac{\mu_j}{r_0}\right)^2 + \left(\frac{\nu_m}{l_0}\right)^2 \tag{7}$$

are the geometrical factors of the mode decay rates, J_0 is the Bessel function and

$$\eta_m = \arctan\frac{\nu_m}{\alpha l_0} = -\frac{\nu_m}{2} - \frac{m+1}{2}\pi. \tag{8}$$

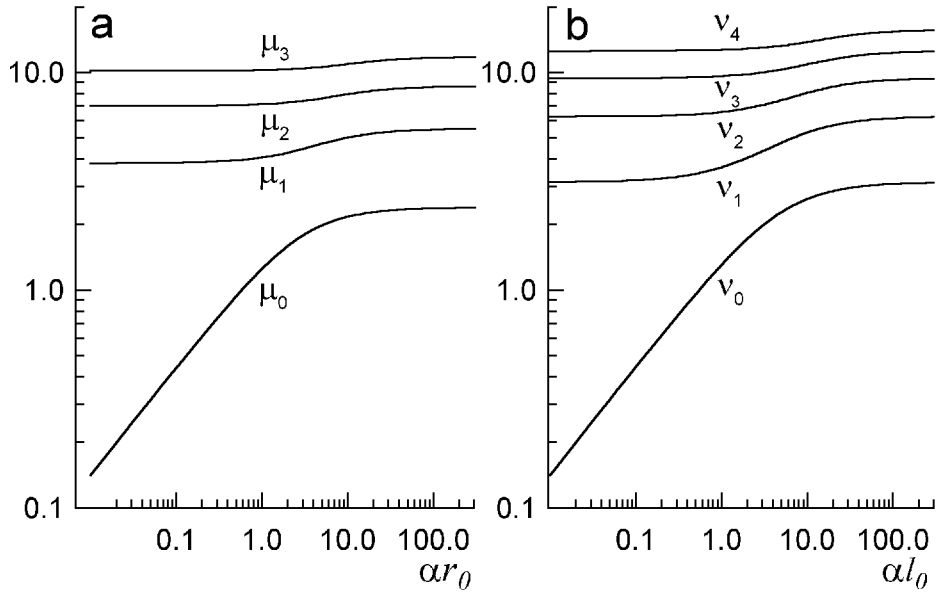

Fig. 2. Dependence of magnitudes of μ_j on αr_0 (a) and ν_m on αl_0 (b).

μ_j and ν_m are the positive roots of the following equations:

$$\mu_j J_0'(\mu_j) + \alpha r_0 J_0(\mu_j) = 0, \tag{9}$$

$$\cot(\nu_m) = \frac{\nu_m^2 - \alpha^2 l_0^2}{2\nu_m \alpha l_0}. \tag{10}$$

In Eq. (6) the coefficients A_{mj} depend on the initial conditions and have the form

$$A_{mj} = \frac{4\pi \int_0^{r_0} \int_0^{l_0} [n(t=0) - n_0]\, r J_0\left(\frac{\mu_j}{r_0} r\right) \sin\left(\frac{\nu_m}{l_0} z + \eta_m\right) \mathrm{d}r\mathrm{d}z}{\pi r_0^2 l_0 \left(1 + \frac{2\alpha l_0}{\alpha^2 l_0^2 + \nu_m^2}\right) [J_0'(\mu_j)]^2 \left(1 + \frac{r_0^2 \alpha^2}{\mu_j^2}\right)}. \tag{11}$$

The coefficients ν_m and μ_j which determine the decay rates in exponential factors in Eq. (6) depend on α and dimensions of the cell. The plots of μ_j on αr_0 and ν_m on αl_0 are shown in Fig. 2.

3. Experimental set-up and data analysis

3.1. Experiment

The cylindrical quartz cells used in the experiment were 10.5 cm long with 15 cm side arm. The smaller cells of 3.7 cm length without a side arm were also used. The inner diameter of both types of the cells was identical and equal 2.8 cm. The side arm made possible controlling the atoms density in the cell independently from the temperature of the main part of the cell while in the smaller cell equilibrium pressure of the Cd vapour was equal to that of saturated vapour at the cell temperature.

All cells were heated up under vacuum. Metallic cadmium was filled in under high vacuum and buffer gas was added at room temperature before detaching the cell from the vacuum system. A special treatment was applied to every cell with the side arm before measurements in order to remove Cd-atoms deposit from the walls. The cell was heated and the side arm was cooled at the same time until the liquid nitrogen temperature was achieved. After the series of measurement another process was applied for every cell, namely the side arm was heated while the rest of the cell was kept at room temperature to insert cadmium atoms into the cell and measurements were repeated under conditions similar to that in the cell without the side arm.

The cell was situated inside a two-part oven which makes possible independent controlling the temperature of the cell and the side arm. Two discharge coils, which produced a pulsing electromagnetic field at frequency about 90 MHz, were installed around the cell. The distance between discharge coils was 1/4 of the cell length (see Fig. 1). The geometry was carefully chosen to ensure axial symmetry of the discharge and inversion symmetry with respect to the centre of the cell. The light source was the commercial dc cadmium spectral lamp (Osram type CD/10). The monochromator was used to separate 326.1 nm intercombination Cd($^1S_0$–$^3P_1$)

line. The intensity of the light passing through the cell was detected by a photomultiplier. In every measurement the size of the detection beam collinear with a cell symmetry axis was determined by diaphragms and optical elements and it was 0.5 cm in diameter. The experimental set-up is shown in Fig. 3.

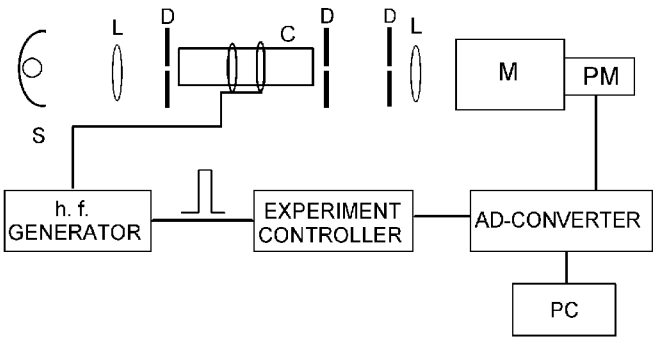

Fig. 3. The experimental set-up (S — Cd spectral lamp, L — lens, D — diaphragm, C — cell, M — monochromator, PM — photomultiplier).

Measurements were performed in the following way. Discharge coils produced pulses of electromagnetic field, at the end of each pulse one started recording the intensity of the light passing through the cell. The change of the light intensity after switching off the discharge due to the changes of Cd atoms concentration caused by the atoms diffusion was named the absorption signal.

The absorption signal was processed by a 12-bit analog-digital converter AD-212 (virtual oscilloscope) PC compatible which made possible averaging over many runs. A proper quality of the signal was attainable after averaging over from 20 to 200 runs depending on buffer gas pressure and experimental conditions. The absorption signal after rf pulse was recorded in 950 points. The rf discharge pulse duration was between 5 and 75 ms, while the repetition period was from 4 to 40 s and it was usually two times longer than the recorded absorption signal.

Assuming i_0 the intensity of the light entering the cell and ξ the absorption cross-section, one obtains the light intensity leaving the cell equal to $i(t) = i_0 \exp(-\xi \int_V n(r,z,t)\mathrm{d}\tau)$. In equilibrium conditions we have $i_\mathrm{e} = i_0 \exp(-\xi \int_V n_0 \mathrm{d}\tau)$. Concentrations n and n_0 are defined in Eq. (6). Assuming a small optical thickness of the discharge plasma the absorption signal $S(t)$ can be described by

$$S(t) = i(t) - i_\mathrm{e} = i_0 \xi \int_V [n_0 - n(r,z,t)]\mathrm{d}\tau = \sum_{m,j} S_{mj} \exp(-D\beta_{mj} t), \qquad (12)$$

where V is a volume of the cell touched by the detection beam and

$$S_{mj} = i_0 \xi \int_V A_{mj} J_0 \left(\frac{\mu_j}{r_0} r\right) \sin\left(\frac{\nu_m}{l_0} z + \eta_m\right) \mathrm{d}\tau. \qquad (13)$$

3.2. The discharge

The initial spatial distribution of Cd atoms produced by pulsed rf discharge depends on many factors such as high frequency field geometry, atoms, ions, and electron collisions in the weakly ionized plasma. In the investigation of the transport processes described by elementary diffusion equation the low Cd atoms gradient was essential.

In the cell with the metal located at the end of the side arm only the Cd gradient occurs due to spatial processes. As a result of the discharge the cadmium atoms are ionized. Electrons and ions diffuse to the walls in a process of ambipolar diffusion and they recombine at the cell walls. Because the coefficient of the ambipolar diffusion is usually one order of magnitude higher than this of neutral atoms, the concentration of atoms becomes smaller in the region of stronger discharge in this case at the centre of the cell. This process produces initial gradient of cadmium atoms. During the discharge pulse absorption decreases because the average concentration of atoms in the region penetrated by detection beam becomes lower after turning the discharge on. After the end of the discharge pulse absorption returns to the level as it was before the discharge. Total difference $i(t) - i_e$ is presented in Fig. 4a. In this case the absorption signal $S(t)$ is above zero.

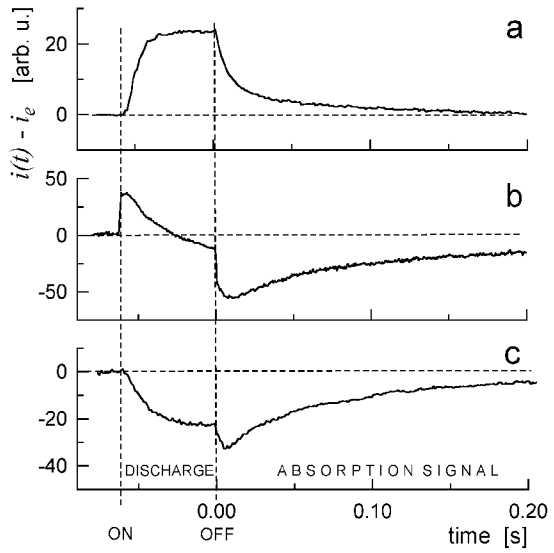

Fig. 4. Total difference $i(t) - i_e$ for 326.1 nm line (details in the text).

In the instance when the atoms are deposited only on the cell walls they are released during the discharge like in the discharge in the hollow cathode lamp and produce the initial atoms gradient. Cadmium atoms diffuse to the detection beam

region during the discharge pulse and in the short time after turning the discharge off (absorption increases). Then the concentration returns to the equilibrium level and absorption decreases. The absorption signal is below zero as shown in Fig. 4c.

In the cell with some deposit on the wall both processes are responsible for initial Cd atoms gradient in different extent as shown in Fig. 4b.

3.3. Data analysis

Data analysis consisted in fitting Eq. (12) to the measured absorption signal using a least-squares method. In order to avoid any effect of the plasma excitation the signal was analysed beginning at the time about 10 ms after termination of the discharge. During that time the quenching of metastable atoms as well as a volume recombination through various reaction channels in weakly ionized plasma occurs. The fitting parameters were S_{mj}, D, and α. As it is seen from Eqs. (9, 10) the magnitudes μ_j and ν_m are the functions of α. Therefore, in order to shorten the computation procedure, the curves presented in Fig. 2a and b were fitted as seven parameter functions in the following form: $\mu_j = a_{j0} + a_{j1}\exp(-b_{j1}\alpha r_0) + a_{j2}\exp(-b_{j2}\alpha r_0) + a_{j3}\exp(-b_{j3}\alpha r_0)$ and $\nu_m = c_{m0} + c_{m1}\exp(-d_{m1}\alpha l_0) + c_{m2}\exp(-d_{m2}\alpha l_0) + c_{m3}\exp(-d_{m3}\alpha l_0)$.

Because $\sin[(\nu_m/l_0)z + \eta_m]$ with odd m in Eq. (6) changes the sign on inversion with respect to the plane through the middle of the cell ($z = l_0/2$) corresponding components S_{mj} will not be present in the signal. It limits the number of observed modes in the absorption signal. Assuming identical boundary conditions

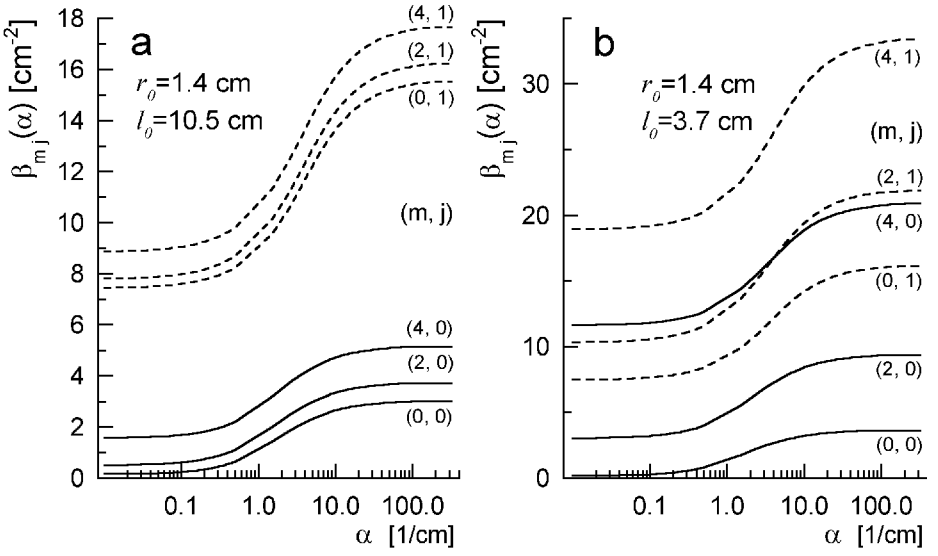

Fig. 5. Dependence of geometrical factors of the mode decay β_{mj} on α for different types of the cell.

on the cell walls (Eq. (2)) reduction of the odd modes will be fulfilled even for axial symmetry only and nonsymmetric atomic density gradient with respect to the centre of the cell produced during a hf discharge.

A number of fitted diffusion modes was usually confined to three with $m = 0$, 2, 4 and $j = 0$. In some cases, especially for higher pressures of buffer gas we could observe in the signal the modes of the group $(m, 1)$. Since the β_{m1} are close to each other for a longer cell (see Fig. 5a), these modes could be treated in the fitting procedure as a single effective additional mode. Nevertheless, the contribution of such a mode as well as mode (0, 1) for a shorter cell (see Fig. 5b) to the signal was found to be negligible. The relative uncertainties of the values D and α fitted in such a way were in the region between 5% and 25% for D and between 8% and 40% for α depending on the experimental conditions.

4. Results and discussion

Measurements were performed for the cells with the side arm containing cadmium and filled with following noble gases under the pressures (reduced to the temperature 273 K): neon (5.5, 8.9, 18.1, 34.5, and 52.7 hPa), argon (6.6, 17.7, and 28.1 hPa), krypton (2.4, 6.7, and 13.1 hPa) and xenon (2.0, 6.0, 6.2 hPa). In the temperature region between 350 and 550 K two series of measurements were performed for 5–10 values of temperature. During the measurement the temperature difference between the cell and side arm was stable and was contained within the limits between 30 and 120 K. The measurements for cadmium with xenon (2.69, 6.7, and 11.2 hPa) as a buffer gas was done also for the short cell (without the side arm).

Typical signals recorded for cadmium with 17.7 hPa of argon for cells without deposit of cadmium atoms on the cell walls are shown in Fig. 6a, while Fig. 6b shows the absorption signals for the same cell in the presence of the deposit on the cell walls.

In the final analysis of the results only those data were chosen for which the relative uncertainties of both D and α are not higher than 25%.

We should emphasize that according to Eq. (5) the knowledge of the magnitude α enables one to determine the coefficient of the reflection R of the cadmium atoms from the wall. In order to determine the value of R we assume in Eq. (5) the classical form of $\lambda = 3D/\overline{v}$, where $\overline{v}$ is the mean velocity of the atoms. The values of R determined in such a way for the cells of a length 10.5 cm containing the mixture of cadmium and neon at pressures 18.1, 34.5, and 52.7 hPa are presented in Fig. 7a, where they are plotted versus the cell temperature T. Figure 7b shows the results of R determined in all measurements, i.e. for all buffer gases: Ne, Ar, Kr, Xe for a longer cell and for Xe as a buffer for a shorter cell plotted versus temperature. It should be noted that for the longer cell the values of the reflection coefficient are close to unity and are located in the region between 0.9990 and 1.0000. The value of the reflection coefficient for the shorter cell are smaller than

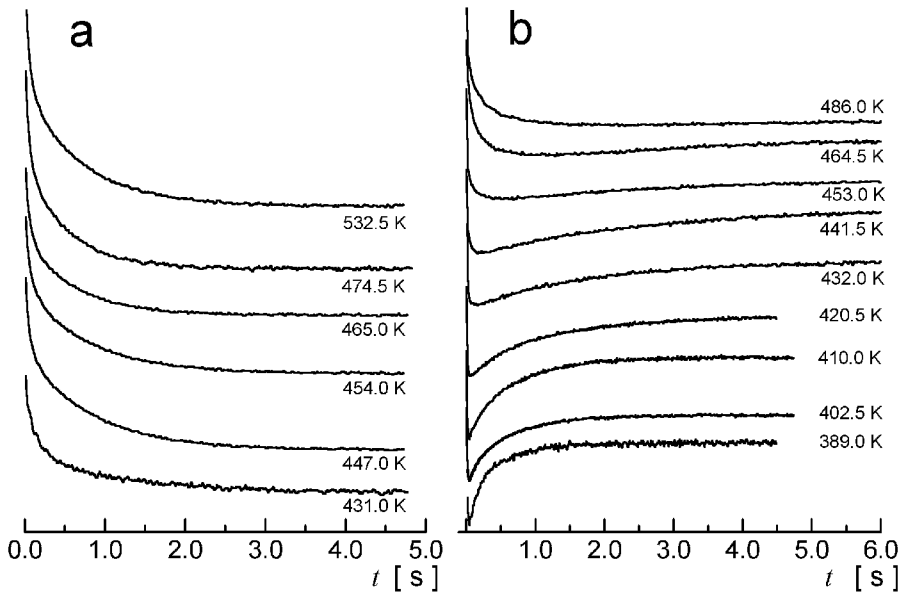

Fig. 6. Typical absorption signals without deposit (a) and with deposit (b) of the Cd atoms on the wall. The temperature difference between the cell and the side arm exceeded 30 K. The pressure of buffer gas (argon) was 17.7 hPa.

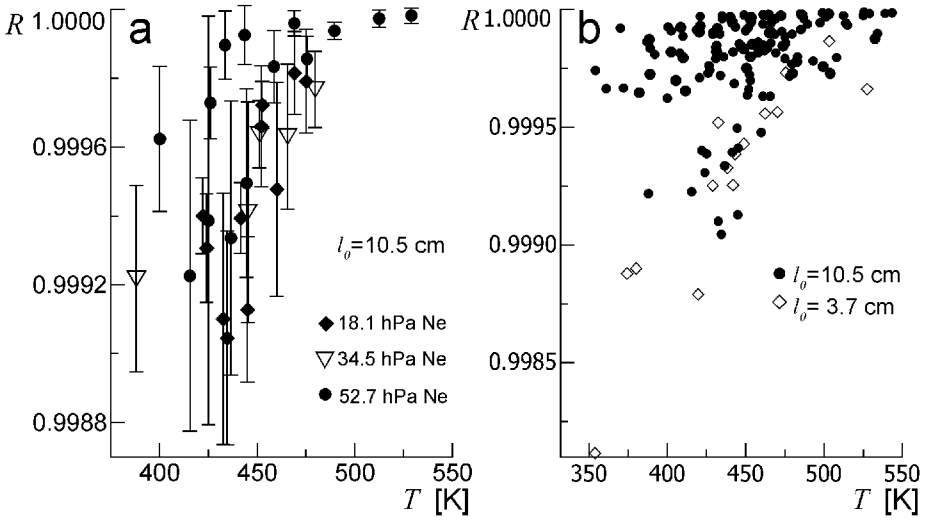

Fig. 7. The value of reflection coefficient against temperature (for explanation see the text).

those for the large ones. We should note that in the limits of experimental uncertainties we have not observed any difference between the values of R determined for "pure" cell, i.e. those without a deposit in the walls, and those determined

for the cells with deposit. For all measurements one can observe the dependence of R on temperature. To our knowledge, the only measurements of the reflection coefficient for the metal atoms are those of Rusinov et al. [5] for the manganese atoms, who reported the values of R contained in the region between 0.60 and 0.88. This coefficient was determined in a segmented hollow cathode discharge at a temperature of 320 K. In their experiment however, the reflection of atoms took place on the metallic wall. The value of R is surprisingly high compared to the one mentioned above. This is the consequence of the way we calculated the value of R using Eq. (5) and the parameter α obtained from fitting Eq. (12) to the signal using a least-squares method. The relative uncertainty of the determined values of

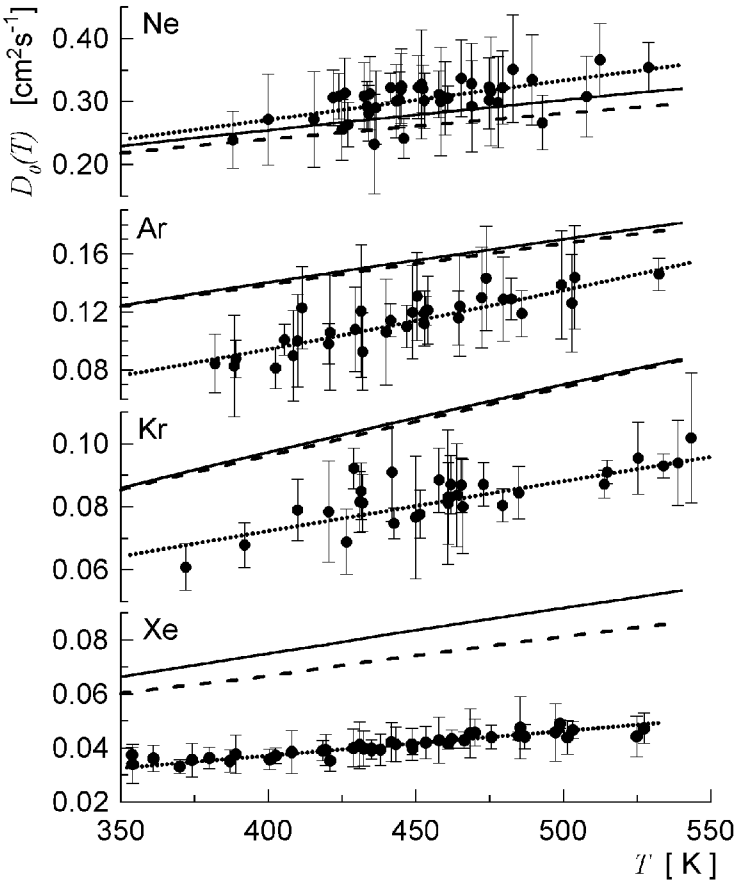

Fig. 8. Experimental and theoretical values of diffusion coefficient together with the fit of Eq. (15): (·····) — the fit of Eq. (15) to the experimental data (•), (– – – –) — theoretical values calculated using a Morse potential with spectroscopic data given by Koperski and Czajkowski [16], (———) — theoretical values calculated using the numerical potential given by Czuchaj and Stoll [15].

the reflection coefficient is then of the order of $(1 - R)$ multiplied by the sum of relative uncertainties of the fitted D and α values.

The values of the diffusion coefficient at the temperature $D_0(T)$ of the cadmium atoms in noble gases (Ne, Ar, Kr, Xe) are shown in Fig. 8, where they are plotted versus the cell temperature T.

To make a comparison of experimentally determined temperature dependence with theoretical one we assumed the relation between diffusion constant and diffusion coefficient in the following form:

$$D(T) = D_0(T)\frac{N_0}{N} = D_0(T_0)\left(\frac{T}{T_0}\right)^{\gamma}\frac{N_0}{N} = D_0(T_0)\left(\frac{T}{T_0}\right)^{\gamma+1}\frac{p_0}{p}, \tag{14}$$

where $D_0(T_0)$ denotes the diffusion coefficient at normal conditions, N is the concentration of buffer gas atoms in the cell and N_0 is the concentration of atoms at the normal conditions. In Eq. (14) we have assumed that

$$D_0(T) = D_0(T_0)\left(\frac{T}{T_0}\right)^{\gamma}. \tag{15}$$

It should be noted that Eq. (15) is strictly valid for the repulsive inverse-power potential $V \sim r^{-m}$ only [13]. In this case $\gamma = 0.5 + 2/m$. $D_0(T_0)$ and γ were determined from the best fit of Eq. (15) to our experimental and theoretical data. Theoretical values of $D_0(T)$ were calculated using the classical Chapman–Enskog approximation which is sufficiently accurate at high temperatures [14]. In our calculation we have used the numerical potentials due to Czuchaj and Stoll [15] and the empirical Morse potential with spectroscopic constants determined by Koper-

TABLE

Values of $D_0(T_0)$ and γ obtained from the best fit of Eq. (15) to the experimental and theoretical dependence of $D_0(T)$. Numbers in parenthesis are standard uncertainties of least-square fit.

Buffer gas	Experiment		Theory	
	$D_0(T_0)$ [cm^2 s^{-1}]	γ	$D_0(T_0)$ [cm^2 s^{-1}]	γ
Ne	0.189(30)	0.93(25)	0.189	$0.771^{\mathrm{Cz-S}}$
			0.182	$0.705^{\mathrm{K-Cz}}$
Ar	0.056(6)	1.40(22)	0.105	$0.864^{\mathrm{Cz-S}}$
			0.100	$0.833^{\mathrm{K-Cz}}$
Kr	0.051(4)	0.89(11)	0.069	$0.895^{\mathrm{Cz-S}}$
			0.068	$0.908^{\mathrm{K-Cz}}$
Xe	0.0253(20)	1.0(1)	0.053	$0.907^{\mathrm{Cz-S}}$
			0.048	$0.852^{\mathrm{K-Cz}}$

$^{\mathrm{Cz-S}}$ numeric potential given by Czuchaj and Stoll [15],
$^{\mathrm{K-Cz}}$ spectroscopic constants for Morse potential given by Koperski and Czajkowski [16].

ski and Czajkowski [16]. The calculation were done for the temperature region between 350 and 550 K. The values of $D_0(T_0)$ and γ determined in this work are listed in Table. Figure 8 indicates that Eq. (15) can reproduce the temperature dependence of the experimental value of $D_0(T)$ for Cd-noble gas-atom systems. On the other hand, the agreement between theoretical and experimental values of $D_0(T)$ is poor except the case of Cd–Ne system. For Cd–Ar, Cd–Kr, and Cd–Xe mixtures the experimental values are smaller than the theoretical ones by 50%, 35%, and 100%, respectively. Moreover one can see that agreement of experimental and theoretical values of γ is good except for the Cd–Ar systems and γ calculated using the Koperski and Czajkowski [16] spectroscopic data for Cd–Xe system.

Acknowledgments

The authors wish to thank prof. A. Bielski for fruitful discussion and critical reading of the manuscript. The authors are also grateful to the Referee for critical remarks and suggestions.

This work was supported by grant No 5 P03B 066 20 (354/P03/2001/20) from the State Committee for Scientific Research.

References

[1] D.W. Ernie, H.J. Oskam, *Phys. Rev. A* **23,** 325 (1981).

[2] N.P. Penkin, T.P. Redko, *Opt. Spectrosk.* **46,** 1078 (1979).

[3] H. Sekido, T. Kondo, A. Kodo, T. Goto, *J. Phys. D, Appl. Phys.* **26,** 1414 (1993).

[4] W. Kwaśniewski, K. Dzięciołowski, T.M. Adamowicz, *Acta Phys. Pol. A* **102,** 747 (2002).

[5] I.M. Rusinov, G.W. Paeva, A.B. Blagoev, *J. Phys. D, Appl. Phys.* **30,** 1878 (1997).

[6] H.J. Cornelissen, *J. Phys. B, At. Mol. Opt. Phys.* **18,** 3445 (1985).

[7] A. Bielski, R. Ciuryło, J. Domysławska, D. Lisak, R.S. Trawiński, J. Szudy, *Phys. Rev. A* **62,** 32511 (2000).

[8] P. Rudecki, *Acta Phys. Pol. A* **100,** 915 (2001).

[9] T. Koga, *Introduction to Kinetic Theory of Stochastic Processes in Gaseous Systems*, Oxford Pergamon Press, 1970.

[10] F. Masnou-Seeuws, M.A. Bouchiat, *J. Phys. (France)* **28,** 406 (1968).

[11] P.J. Chantry, *J. Appl. Phys.* **62,** 1141 (1987).

[12] S. Suzuki, H. Itoh, N. Ikuta, H. Sekizawa *J. Phys. D, Appl. Phys.* **25,** 1568 (1992).

[13] S. Chapman, T.G. Cowling, *The Mathematical Theory of Non-Uniform Gases*, Cambridge Press, Cambridge 1970.

[14] J.O. Hirschfelder, Ch.F. Curtiss, R.B. Bird, *Molecular Theory of Gases and Liquids*, Wiley, New York 1964.

[15] E. Czuchaj, H. Stoll, *Chem. Phys.* **248,** 1 (1999).

[16] J. Koperski, M. Czajkowski, *J. Chem. Phys.* **109,** 459 (1998).